Lecture 2

Recall the following

$S_{fi} = \langle f|S|i\rangle$ $\qquad \sum_n S^{\dagger}_{fn} S_{ni} = \delta_{fi}$ $\qquad S = 1 + iT$

$\Rightarrow \quad T - T^{\dagger} = i T^{\dagger} T$ $\qquad \mathrm{Im}\, T_{fi} = \frac{1}{2} \sum_n T^{\dagger}_{fn} T_{ni}$

Martin and Spearman $\qquad$ electron-pion scattering

Scattering

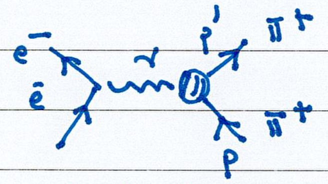

$q = p' - p$

$\langle p' | j_\mu | p \rangle = (p_\mu + p'_\mu)\, F(t)$ $\qquad F(0) = 1$

$t \equiv -q_\mu q^\mu$ $\qquad$ [Note metric p.37 fn
$p_\mu p^\mu = -p_0^2 + p^2$

$t \leq 0$ range for
e-π scattering

$$t \equiv -q_\mu q^\mu = -(p_\mu + p'_\mu)^2 \geqslant 4m^2$$

related to production $e^- + e^+ \to \pi^+ + \pi^+$

Production

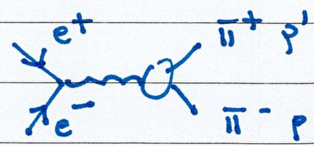

Cauchy's thm applied to

$\frac{F(t') - F(0)}{t'(t' - t)}$ to give $F(t) = 1 + \frac{t}{\pi} \int_{4m^2}^{\infty} \frac{\mathrm{Im}\, F(t')\, dt'}{t'(t' - t)}$

$\mathrm{Im}\, F(t) = \frac{1}{2i} \left[F(t + i\varepsilon) - F(t - i\varepsilon) \right]$ $\qquad$ (real analytic)
F(t)

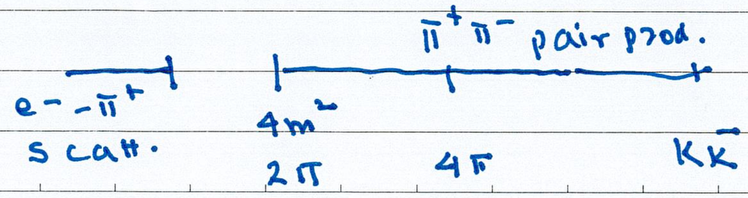

Dispersion relations are more meaningful taking into account unitarity

$$\mathrm{Im}\, F(t) = \mathrm{Im} \langle \pi^+ \pi^+ | T | \gamma \rangle$$

$$= \sum_n \langle \pi^- \pi^+ | T^+ | n \rangle \langle n | T | \gamma \rangle$$

sum over all physical states

Im 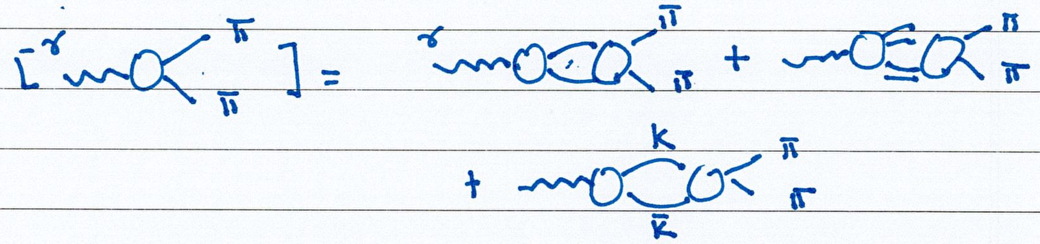

First diagram gives $\mathrm{Im}\, F(t) \sim T^*_{\pi\pi} F(t)$

Our examples in CHPT so far.

E-M ff of the pion Donoghue et al.

$$H(a) = -\int_0^1 dx \ln(1 - ax(1-x)) \quad \text{same as}$$

$$16\pi^2 \bar{J}(s) = \left\{ \sigma(s) \ln\left(\frac{\sigma(s)-1}{\sigma(s)+1}\right) + 2 \right\}$$

$$\mathrm{Im}\, \bar{J}(s) = \frac{1}{16\pi} \sigma(s) \, \theta(s-4) \qquad \sigma(s) = \sqrt{1 - \frac{4m^2}{s}}$$

$(m=1)$

Easy to verify $\bar{J}(s) = \bar{J}(0) + \frac{1}{\pi} \int_{4m^2}^{\infty} \frac{\mathrm{Im}\, \bar{J}(s')}{s'(s'-s)} ds'$

Scalar form factor

Tree  1-loop: 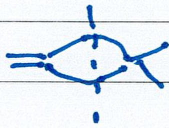  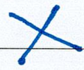

Γ_{tree} $\quad$ $\pi-\pi$ tree

$I = 0$

$$\bar{\Gamma}(s) = 1 + \frac{s}{16\pi F_\pi^2}(\bar{l}_4 - 1) + \frac{2s - M_\pi^2}{2F_\pi^2}\bar{J}(s) \qquad l = 0$$

e.m. form factor

Tree 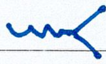 1-loop 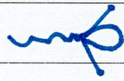 

 

tree $\quad$ $\pi-\pi$ tree

$$1 + \text{polynomial pieces} + \frac{1}{96\pi^2}(q^2 - m_\pi^2)\, H(q^2/m_\pi^2) \qquad I = 1,\ l = 1$$

This brings us to $\pi-\pi$ amplitudes.

Nb shows 2-loop unitarity relation for form factor

Chiral extrapolation of hadronic vacuum polarization

Gilberto Colangelo[a], Martin Hoferichter[a], Bastian Kubis[b], Malwin Niehus[b], Jacobo Ruiz de Elvira[a]

[a]*Albert Einstein Center for Fundamental Physics, Institute for Theoretical Physics, University of Bern, Sidlerstrasse 5, 3012 Bern, Switzerland*
[b]*Helmholtz-Institut für Strahlen- und Kernphysik (Theorie) and Bethe Center for Theoretical Physics, Universität Bonn, 53115 Bonn, Germany*

Abstract

We study the pion-mass dependence of the two-pion channel in the hadronic-vacuum-polarization (HVP) contribution to the anomalous magnetic moment of the muon a_μ^{HVP}, by using an Omnès representation for the pion vector form factor with the phase shift derived from the inverse-amplitude method (IAM). Our results constrain the dominant isospin-1 part of the isospin-symmetric light-quark contribution, and should thus allow one to better control the chiral extrapolation of a_μ^{HVP}, required for lattice-QCD calculations performed at larger-than-physical pion masses. In particular, the comparison of the one- and two-loop IAM allows us to estimate the associated systematic uncertainties and show that these are under good control.

1. Introduction

Currently the biggest uncertainty in the Standard-Model prediction for the anomalous magnetic moment of the muon [1–28]

$$a_\mu^{\text{SM}} = 116\,591\,810(43)\times 10^{-11} \qquad (1)$$

resides in the HVP contribution, which, when derived from $e^+e^- \to$ hadrons cross-section data [1, 6–12]

$$a_\mu^{\text{HVP}}\big|_{e^+e^-} = 6\,931(40)\times 10^{-11}, \qquad (2)$$

leads to a 4.2σ difference to experiment [29–33]

$$a_\mu^{\text{exp}} = 116\,592\,061(41)\times 10^{-11}. \qquad (3)$$

Improving the (time-like) data-driven evaluation of HVP (2) relies on new data, most crucially for the $e^+e^- \to 2\pi$ channel [34, 35], while a space-like measurement would be possible at the MUonE experiment [36, 37].

Alternatively, the precision of the HVP contribution evaluated in lattice QCD is getting closer to the data-driven determination, with an average [1] (based on Refs. [38–46])

$$a_\mu^{\text{HVP}}\big|_{\text{lattice average}} = 7\,116(184)\times 10^{-11}, \qquad (4)$$

and a subsequent first sub-percent result [47]

$$a_\mu^{\text{HVP}} = 7075(55)\times 10^{-11}. \qquad (5)$$

In this Letter, we do not address the 2.1σ tension with the data-driven approach,[1] see Refs. [56–60], but instead focus on the potential source of systematic uncertainty in lattice calculations that may arise if the simulation is performed at unphysical values of the quark masses.

This effect is most relevant for the isospin-symmetric *ud* correlator, both because its contribution is by far the largest, and because it is the lightest quarks that make simulations at the physical point expensive. Often, the required quark-mass extrapolation can be controlled using chiral perturbation theory (ChPT), at least for sufficiently small masses, but the analysis of Ref. [61] showed that for the HVP contribution this does not seem to be the case. On the one hand, the presence of a mass scale lighter than M_π, namely the muon mass, makes the pure chiral expansion of practical use only for $M_\pi \ll m_\mu$ [61]. Physically, it is well known that the 2π contribution to HVP is dominated by the $\rho(770)$ meson, see, e.g., Ref. [62] for the implication for lattice calculations, and that controlling the quark-mass dependence of its parameters requires information beyond ChPT. On the other hand, one would not expect the quark-mass dependence of the $\rho(770)$ mass, for example, to be so complicated that it could not be described by a simple parameterization. If this is the case, it is not clear why a simple parameterization of the quark-mass dependence of the 2π contribution to HVP should not be possible, and even allow for a controlled chiral extrapolation of good precision (in fact, finite-volume corrections have been addressed using ChPT methods [63]). Given the high computational cost of simulations at the physical quark masses this is a question of current high interest, which can be addressed from a ChPT/phenomenological point of view and deserves the detailed investigation we aim to provide in this Letter.

Our approach here is to follow Ref. [64] and combine an Omnès description [65] of the pion vector form factor (VFF) with the inverse-amplitude method (IAM) [66–73], to capture the quark-mass dependence of the dominant two-pion intermediate states. To this end, we employ the one- and two-loop IAM to describe the pion-mass dependence of the $\pi\pi$ P-wave phase shift [74], leading to a representation that guides the chiral extrapolation of the $I = 1$ component of the isospin-symmetric *ud* contribution to a_μ^{HVP}. We stress that our goal is not to show that the IAM is able to *predict* to high precision the quark-mass

[1]In contrast, there is good agreement between data-driven and lattice-QCD evaluations for hadronic light-by-light scattering, as further corroborated by recent work [48–55].

Pion Form Factor Phase, $\pi\pi$ Elasticity and New e^+e^- Data

S. Eidelman [a] and L. Łukaszuk [b]

[a] *Budker Institute of Nuclear Physics, Acad. Lavrentyev 11, Novosibirsk, 630090, Russia*

[b] *Andrzej Sołtan Institute for Nuclear Studies, Hoża 69, PL-00-681, Warsaw, Poland*

Abstract

New precise data on the low energy e^+e^- annihilation into hadrons from Novosibirsk are used to obtain bounds on the elasticity parameter and the difference between the phase of the pion form factor and that of the $\pi\pi$ scattering.

Pion form factor and its relation to $\pi\pi$ scattering have been extensively studied for many years (see [1] and references therein). Although the form factor phase naturally appears in any model of the pion form factor [2, 3, 4, 5, 6], it is well known that only the absolute value of the form factor can be usually measured while information on the phase can be gained from sophisticated interference experiments. However, as shown long ago, there is an interesting possibility to obtain bounds on the elasticity parameter of the P-wave $\pi\pi$ scattering, η_1, and the difference between the phase of the pion form factor ψ and that of the $\pi\pi$ scattering δ_1 in a model-independent way under very general assumptions [7]. Namely, the following inequality has been obtained there [1] :

$$(\frac{1-\eta_1}{2})^2 + \eta_1 \sin^2(\psi - \delta_1) \leqslant \frac{1-\eta_1^2}{4} \cdot r, \qquad 0 \leqslant \eta_1 \leqslant 1 \tag{1}$$

or, equivalently,

$$|a(\eta_1, \psi - \delta_1)|^2 \leqslant \frac{1-\eta_1^2}{4} \cdot r \tag{2}$$

[1] A factor $|F|^2$ was unfortunately omitted on l.h.s. of formula (5a) in Ref. [7]. All other relations in Ref. [7] are correct.

Preprint submitted to Elsevier Science

Brings us to $\pi - \pi$ amplitudes

(Martin, Morgan and Shaw)

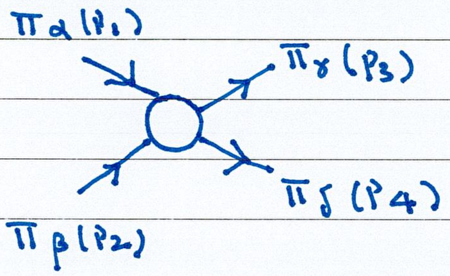

$$s \equiv -(p_1+p_2)^2 = -(p_3+p_4)^2$$

$$t \equiv -(p_1-p_3)^2 = -(p_2-p_4)^2$$

$$u \equiv -(p_1-p_4)^2 = -(p_2-p_3)^2$$

$$s+t+u = 4\mu^2$$

Physical region for s-channel scattering

$$s \geq 4m^2, \; t \leq 0, \; u \leq 0$$

$$q_s^2 = \frac{s-4m^2}{4} \qquad t = -2q_s^2(1-\cos\theta_s)$$

$$\cos\theta_s = \frac{t-u}{4q_s^2} = \frac{t-u}{s-4\mu^2}$$

$$P_1 = (E, |\vec{p}|, 0, 0) \qquad |\vec{p}| = p$$
$$P_2 = (E, -|\vec{p}|, 0, 0)$$

$$P_3 = (E, p\cos\theta, p\sin\theta, 0)$$
$$P_4 = (E, -p\cos\theta, -p\sin\theta, 0)$$

$$s = 4E^2 \qquad E^2 - p^2 = m^2 ; \; p^2 = E^2 - m^2$$
$$= \frac{s}{4} - m^2$$
$$= \frac{s - 4m^2}{4}$$

$$t = -\left(p^2(1-\cos\theta)^2 + p^2\sin^2\theta\right)$$
$$= -\left(p^2 - 2p^2\cos\theta + p^2\right)$$
$$= -\left(2p^2 - 2p^2\cos\theta\right)$$
$$= -2p^2(1-\cos\theta)$$

$$u = -2p^2(1+\cos\theta)$$

$$t - u = +4p^2\cos\theta$$

$$\cos\theta = \frac{t-u}{4p^2} = \frac{t-u}{s-4m^2}.$$

Next we will introduce the partial wave expansion.

$$T_s^I(s,t,u) = \sum (2l+1)\, P_l(\cos\theta_s)\, T_l^I(s)$$

I – definite iso-spin in the s-channel

$P_l(z)$ – Legendre polynomials

$$\int_{-1}^{1} P_l(z)\, P_{l'}(z)\, dz = \frac{2}{(2l+1)}$$

$$P_0(z) = 1 \qquad P_1(z) = z \qquad P_2(z) = \frac{1}{2}(3z^2-1)$$

$$P_3(z) = \frac{1}{2}(5z^3 - 3z)$$

$$T_s^I(s,t,u) = \lim_{\varepsilon\to 0} T(s+i\varepsilon, t, u)$$

obtained by projection.

- $T_l^I(s)$ – partial wave amplitude complex above $4m^2$

$l = 0$ S-wave

$l = 1$ P-wave

$l = 2$ D-wave

$l = 3$ F-wave

- Narrow-width:

$$\mathrm{Im}\, T_l^I(x) = \sqrt{\frac{x}{x-4m^2}}\; \pi\, \Gamma_m^{\pi\pi} M_m\, \delta(x - M_m^2)$$

In π-π scattering $I = 0, 2$; $l = 0, 2, 4, \ldots$

$I = 1$, $l = 1, 3, 5, \ldots$

(generalized Bose statistics)

Iso-spin and crossing

$$T(s,t,u) = A(s,t,u)\,\delta_{\alpha\beta}\delta_{\gamma\delta} + A(t,u,s)\,\delta_{\alpha\gamma}\delta_{\beta\delta}$$
$$+ A(u,s,t)\,\delta_{\alpha\delta}\delta_{\beta\gamma}$$

$$A(s,t,u) = A(t,u,s) \quad \text{(generalized Bose statistics)}$$

$$T_s^{I=0}(s,t,u) = 3A(s,t,u) + A(t,u,s) + A(u,s,t)$$
$$T_s^{I=1}(s,t,u) = A(t,u,s) - A(u,s,t)$$
$$T_s^{I=2}(s,t,u) = A(t,u,s) - A(u,s,t)$$

Obtained by use of projectors given in Burkhardt

$$P_0^{(s)} = \frac{1}{3}\delta_{\alpha\beta}\delta_{\gamma\delta}$$

$$P_1^{(s)} = \frac{1}{2}[\delta_{\alpha\delta}\delta_{\beta\gamma} - \delta_{\alpha\gamma}\delta_{\beta\delta}]$$

$$P_2^{(s)} = \frac{1}{2}[\delta_{\alpha\delta}\delta_{\beta\gamma} + \delta_{\alpha\gamma}\delta_{\beta\delta}] - \frac{1}{3}\delta_{\alpha\beta}\delta_{\gamma\delta}$$

$$P_0^{(s)} + P_1^{(s)} + P_2^{(s)} = \delta_{\alpha\delta}\delta_{\beta\gamma}$$

One can have projectors for t and u channels

Construct amplitudes of definite iso-spin in t and u channels

Alternatively we can cross from one channel to the other.

By using crossing matrices.

$$C_{st} = \begin{bmatrix} 1/3 & 1 & 5/3 \\ 1/3 & 1/2 & -5/6 \\ 1/3 & -1/2 & 1/6 \end{bmatrix} \qquad C_{su} = \begin{bmatrix} 1/3 & -1 & 5/3 \\ -1/3 & 1/2 & 5/6 \\ 1/3 & 1/2 & 1/6 \end{bmatrix}$$

$$C_{tu} = \begin{bmatrix} 1 & 0 & 0 \\ 0 & -1 & 0 \\ 0 & 0 & 1 \end{bmatrix}$$

Can also be obtained from
Wigner 9-J symbols

$$\begin{pmatrix} I_1 & I_2 & I_{12} \\ I_3 & I_4 & I_{34} \\ I_{13} & I_{24} & I \end{pmatrix} \qquad \begin{aligned} I_{12} &= I_{34} = I_s \\ I_{13} &= I_{24} = I_t \\ I &= 0 \end{aligned}$$

$\pi - \pi$

$I_1 = I_2 = I_3 = I_4 = 1$ $\quad \downarrow \; I = 0$

$\pi - K$

$I_1 = I_3 = 1$

$I_2 = I_4 = 1/2$

and permutations

6-J symbols

Given by Neville

our code does everything

various nbs.

Addition of angular momenta

Addition rule for addition of 2 angular momenta j_1 & j_2

$j = |j_1 - j_1|$ or $j_1 + j_2$

Next system with 0 angular momentum consisting of 3 particles with angular momentum j_1, j_2, j_3 components m_1, m_2, m_3.

Condition $m_1 + m_2 + m_3 = 0$

j_1, j_2, j_3 satisfy vector addition

$|j_1 - j_2| \leq j_3 \leq j_1 + j_2$

$j_1 + j_2 + j_3$ is an integer.

wave function
$$\psi_0 = \sum_{m_1, m_2, m_3} \begin{pmatrix} j_1 & j_2 & j_3 \\ m_1 & m_2 & m_3 \end{pmatrix} \psi^{(1)}_{j_1 m_1} \psi^{(2)}_{j_2 m_2} \psi^{(3)}_{j_3 m_3}$$

can be chosen real

3-j symbol

$\neq 0$ if $m_1 + m_2 + m_3 = 0$

Symmetry properties follow

Relation to C-G coefficients.

$$\langle m_1 m_2 | j m \rangle = (-1)^{j_1 - j_2 + m} (2j+1)^{1/2} \begin{pmatrix} j_1 & j_2 & j \\ m_1 & m_2 & -m \end{pmatrix}$$

Now let us illustrate with chiral amplitude

$$A(s,t,u) = \frac{s - M_\pi^2}{32\pi F_\pi^2}$$

$$T^0(s,t,u) = \frac{2s - \cancel{4} M_\pi^2}{32\pi F_\pi^2}$$

← appears in scalar f.f. unitarity relation

$$= \frac{1}{32\pi F_\pi^2}\left(7\,m_\pi^2 + 8q^2\right) P_0(\cos\theta)$$

Introduce the threshold expansion

$$\mathrm{Re}\, f^I_\ell(s) = q^{2\ell}\left(a^I_\ell + b^I_\ell q^2 + \dots\right)$$

↑ scattering length ↖ effective range

appears in e.m. f.f unitarity

$$T^1(s,t,u) = \frac{t-u}{32\pi F_\pi^2} = \frac{(s-4m_\pi^2)}{96\pi F_\pi^2} \times 3 \cdot \frac{(t-u)}{(s-4m_\pi^2)}$$

$$= \frac{4q^2 \times 3 P_1(\cos\theta)}{96\pi F_\pi^2}$$

Read off the threshold parameters.

$$a^0_0 = \frac{7 M_\pi^2}{32\pi F_\pi^2} \qquad b^0_0 = \frac{M_\pi^2}{4\pi F_\pi^2} \qquad a^1_1 = \frac{1}{24\pi F_\pi^2}$$

At NLO corresponding unitarity relation.

$$\mathrm{Im}\, f^0_0(s) = \frac{\rho(s)}{1024\pi^2 F_\pi^4} (2s - m_\pi^2)^2 \qquad \rho(s) = \sqrt{\frac{s-4}{s}}$$

$$(= \sigma(s))$$

$$\mathrm{Im}\, f^1_1(s) = \frac{\rho(s)}{9216\,\pi^2 F_\pi^4} (s - 4m_\pi^2)^2$$

$$\mathrm{Im}\, f^2_0(s) = \frac{\rho(s)}{1024\,\pi^2 F_\pi^4} (s - 2m_\pi^2)^2$$

No higher waves present at this order with imaginary parts. Persists to next order as well.

At NLO the structure is

$$A(s,t,u) = \Big[\frac{1}{3} W_0(s) + \frac{3}{2}(s-u)\, W_1(t) + \frac{3}{2}(s-t)\, W_1(u)$$
$$+ \frac{1}{2}\Big(W_2(t) + W_2(u) - \frac{2}{3} W_2(s)\Big) \Big]$$

Chiral amplitude contains

$$W_0(s) \quad \frac{3}{32\pi} \quad \frac{2}{2F_\pi^4} \quad (s - 1/2)^2\, \bar{J}(s) \qquad m_\pi = M_\pi = 1$$

$$W_1(s) \quad \frac{1}{576\pi F_\pi^4} (s-4)\, \bar{J}(s)$$

$$W_2(s) \quad \frac{1}{64\pi F_\pi^4} (s-2)^2\, \bar{J}(s)$$

Table 1: Threshold parameters that are relevant in K_{e4} experiments, in units of M_{π^+}.

	Soft pions	Experiment	Improved low energy theorems	size of correction 3:1
a_0^0	0.16	0.26 ± 0.05	0.20 ± 0.005	1.28
b_0^0	0.18	0.25 ± 0.03	0.25 ± 0.02	1.37
a_1^1	0.030	0.038 ± 0.002	0.038 ± 0.003	1.26
b_1^1			$(5 \pm 3) \times 10^{-3}$	

determined by measuring the D-wave scattering lengths a_2^0 and a_2^2 [1],

$$
\begin{aligned}
\bar{l}_1 &= 480\pi^3 F_\pi^4(-a_2^0 + 4a_2^2) + 49/40 + O(M_\pi^2) , \\
\bar{l}_2 &= 480\pi^3 F_\pi^4(a_2^0 - a_2^2) + 27/20 + O(M_\pi^2) ,
\end{aligned}
$$

whereas the constant $\bar{l}_4$ is related to the scalar radius of the pion [1],

$$
\bar{l}_4 = \frac{13}{12} + \frac{8\pi^2 F_\pi^2}{3}\langle r^2\rangle_S^\pi + O(M_\pi^2) .
$$

The S- and P-wave threshold parameters are

$$
\begin{aligned}
a_0^0 &= \frac{7M_\pi^2}{32\pi F_\pi^2}\left\{1 + \frac{M_\pi^2}{3}\langle r^2\rangle_S^\pi + \frac{200\pi F_\pi^2 M_\pi^2}{7}(a_2^0 + 2a_2^2) - \frac{M_\pi^2}{672\pi^2 F_\pi^2}(15\bar{l}_3 - 353) + O(M_\pi^4)\right\} , \\
b_0^0 &= \frac{1}{4\pi F_\pi^2}\left\{1 + \frac{1}{3}M_\pi^2\langle r^2\rangle_S^\pi + 40\pi F_\pi^2 M_\pi^2(a_2^0 + 5a_2^2) + \frac{39M_\pi^2}{64\pi^2 F_\pi^2} + O(M_\pi^4)\right\} , \\
a_1^1 &= \frac{1}{24\pi F_\pi^2}\left\{1 + \frac{1}{3}M_\pi^2\langle r^2\rangle_S^\pi + 80\pi F_\pi^2 M_\pi^2(a_2^0 - \frac{5}{2}a_2^2) + \frac{19M_\pi^2}{576\pi^2 F_\pi^2} + O(M_\pi^4)\right\} , \\
b_1^1 &= \frac{7}{2160\pi^3 F_\pi^4} + \frac{10}{3}(a_2^0 - \frac{5}{2}a_2^2) + O(M_\pi^2) .
\end{aligned}
\tag{2}
$$

The numerical values obtained by evaluating these improved low energy theorems are given in table 1 (in units of M_{π^+}). In column 2 we give the soft pion predictions of Weinberg [12], obtained from the terms proportional to F_π^{-2} in Eq. (2). The third column contains the results of an analysis of the data as reported by Petersen in the compilation of coupling constants and low-energy parameters [8]. The entries in the fourth column correspond to the representation (2). Here, we have used the experimental D-wave scattering lengths and the scalar radius of the pions as an input, together with the value for $\bar{l}_3$ determined in [1][1].

<u>Remark:</u> The errors quoted in column 4 are obtained by adding the uncertainties in $\langle r^2\rangle_S^\pi$, a_2^0, a_2^2 and in $\bar{l}_3$ in quadrature. They measure the accuracy, to which the first order corrections can be calculated, and do not include an estimate of the contributions due to higher order terms. Work to determine those reliably is in progress [11]. Note also, that the S-wave scattering lengths vanish in the chiral limit and we therefore have to expect relatively large electromagnetic corrections to these quantities. To illustrate: if we use the mass of the neutral pion rather than M_{π^+}, the prediction for a_0^0 is lowered by 0.016 (at a fixed value of $\bar{l}_{1,2,3,4}$). <u>End of remark.</u>

Turning now to the energy dependence of the phase shifts, we note that these may be worked out from the explicit expression for the scattering amplitude given above by use of [13]

$$
\delta_l^I(s) = (1 - 4M_\pi^2/s)^{1/2}\,\mathrm{Re}\, t_l^I(s) + O(E^6) .
$$

[1] To be more specific, we use $\langle r^2\rangle_S^\pi = 0.60 \pm 0.05\,\mathrm{fm}^2$ [7], $\bar{l}_3 = 2.9 \pm 2.4$ [1], $a_2^0 = (17 \pm 3) \cdot 10^{-4} M_\pi^{-4}$ [8], $a_2^2 = (1.3 \pm 3) \cdot 10^{-4} M_\pi^{-4}$ [8], $M_\pi = 139.57$ MeV [10], $F_\pi = 92.4$ MeV [10].

In the following, we concentrate on the phase shift difference

$$
\Delta = \delta_0^0 - \delta_1^1 ,
$$

and obtain

$$
\begin{aligned}
\Delta &= \Delta^{(2)} + \Delta^{(4)} + O(E^6) , \\
\Delta^{(2)} &= \frac{\rho M_\pi^2}{96\pi F_\pi^2}(5x + 1) , \\
\Delta^{(4)} &= \rho M_\pi^4 \left\{ \frac{h(x)}{55296\rho^4 x^2 \pi^3 F_\pi^4} + \frac{(5x-1)\langle r^2\rangle_S^\pi}{288\pi F_\pi^2} + \frac{5}{48}(x^2 + 8x + 12)a_2^0 \right. \\
&\quad \left. + \frac{25}{48}(7x^2 - 28x + 24)a_2^2 - \frac{5\bar{l}_3}{1024\pi^3 F_\pi^4} \right\} ,
\end{aligned}
\tag{3}
$$

where

$$
\begin{aligned}
h(x) &= \rho^2(689x^3 - 4630x^2 + 11396x - 15240)x \\
&\quad 6\rho(50x^4 - 460x^3 + 1319x^2 - 1028x - 112)h_1(x) \\
&\quad +36(3x^2 - 36x + 106)h_1^2(x) , \\
h_1(x) &= \ln\left\{\frac{1-\rho}{1+\rho}\right\} ; \quad \rho = (1 - 4/x)^{1/2} , \quad x = s/M_\pi^2 .
\end{aligned}
\tag{4}
$$

The quantity $\Delta^{(2)}$ stems from the leading order term $(s - M_\pi^2)/F_\pi^2$ in Eq. (1). Numerical results are displayed in the figures. In Fig. 1, we show the data from Ref. [4], together with the full one-loop result $\Delta = \Delta^{(2)} + \Delta^{(4)}$ (solid line) and the leading order term $\Delta^{(2)}$ (dashed line). In Fig. 2, the various contributions to the next-to-leading order term $\Delta^{(4)}$ are resolved. Notice that the contribution from the low-energy constant $\bar{l}_3$ is very small.

For a discussion of the $\pi\pi$ amplitude in the framework of generalized chiral perturbation theory, see Ref. [14].

4 Improvements at DAΦNE

According to Baillargeon and Franzini [3], DAΦNE will allow one to determine the phase shift difference $\delta_0^0 - \delta_1^1$ with considerably higher precision than available now [4]. It will, therefore, be of considerable interest to confront the above predictions with these data. In particular, we note that a value of $a_0^0 = 0.26$ is not compatible with the chiral prediction $a_0^0 = 0.20$.

Acknowledgements

I thank Heiri Leutwyler for informative discussions.

Nb shows 2-loop unitarity

Two-Loop Analysis of the Pion Mass Dependence of the ρ Meson

Malwin Niehus,[1,*] Martin Hoferichter,[2,3,†] Bastian Kubis,[1,‡] and Jacobo Ruiz de Elvira[2,§]
[1]*Helmholtz-Institut für Strahlen- und Kernphysik (Theorie) and Bethe Center for Theoretical Physics, Universität Bonn, 53115 Bonn, Germany*
[2]*Albert Einstein Center for Fundamental Physics, Institute for Theoretical Physics, University of Bern, Sidlerstrasse 5, 3012 Bern, Switzerland*
[3]*Institute for Nuclear Theory, University of Washington, Seattle, Washington 98195-1550, USA*

(Received 11 September 2020; accepted 2 February 2021; published 12 March 2021)

Analyzing the pion mass dependence of $\pi\pi$ scattering phase shifts beyond the low-energy region requires the unitarization of the amplitudes from chiral perturbation theory. In the two-flavor theory, unitarization via the inverse-amplitude method (IAM) can be justified from dispersion relations, which is therefore expected to provide reliable predictions for the pion mass dependence of results from lattice QCD calculations. In this work, we provide compact analytic expression for the two-loop partial-wave amplitudes for $J = 0, 1, 2$ required for the IAM at subleading order. To analyze the pion mass dependence of recent lattice QCD results for the P wave, we develop a fit strategy that for the first time allows us to perform stable two-loop IAM fits and assess the chiral convergence of the IAM approach. While the comparison of subsequent orders suggests a breakdown scale not much below the ρ mass, a detailed understanding of the systematic uncertainties of lattice QCD data is critical to obtain acceptable fits, especially at larger pion masses.

DOI: 10.1103/PhysRevLett.126.102002

Introduction.—While recent years have shown significant progress in understanding the QCD resonance spectrum from first principles in lattice QCD [1], most calculations are still performed at unphysically large pion masses, requiring an extrapolation to the physical point to make connection with experiment. Such extrapolations can be controlled using effective field theories, i.e., chiral perturbation theory (ChPT) [2–4] for observables that allow for a perturbative expansion. By definition, this precludes a direct application to resonances such as the ρ meson in the P wave of $\pi\pi$ scattering. In fact, spectroscopy results from lattice QCD are arguably most advanced for the ρ meson [5–20], with even calculations at the physical point now available [20], which makes this channel the ideal example to study the details of the pion mass dependence. In addition, the $\pi\pi$ P wave features prominently in a host of phenomenological applications, among them hadronic vacuum polarization [21–26], nucleon form factors [27–30], and the radiative process $\gamma\pi \to \pi\pi$ [31,32]. For the latter, a thorough understanding of the $\pi\pi$ P wave is prerequisite for an analysis of the pion mass dependence of recent lattice results [33–35], see Ref. [36], and similarly for decays into three-pion final states [37].

On the technical level, the failure to produce resonant states is related to the fact that unitarity is only restored perturbatively in ChPT, so that any description of resonances requires a unitarization procedure. A widely used approach known as the inverse-amplitude method (IAM) achieves this unitarization by studying the unitarity relation for the inverse amplitude [38–46]. In particular, in the case of SU(2) ChPT the IAM procedure can be derived starting from a dispersion relation in which the discontinuity of the left-hand cut is approximated by its chiral expansion [41,42]. While Adler zeros induce a modification for the S waves [47], the naive derivation of the IAM survives for the P-wave amplitude: writing the partial wave for $\pi\pi$ scattering $t(s)$ as

$$t(s) = t_2(s) + t_4(s) + t_6(s), \tag{1}$$

with the subscripts indicating the chiral order, the unitarized amplitude at next-to-leading order (NLO) becomes [39–41]

$$t_{\rm NLO}(s) = \frac{[t_2(s)]^2}{t_2(s) - t_4(s)}, \tag{2}$$

while at next-to-next-to-leading order (NNLO) [42,45]

Let us study the analytic properties of form factors a bit more combined with unitarity.

$F(t)$ as defined by I. Caprini

In the elastic region $\mathrm{Im}\, F(t) = \rho(t)\, f_1^1(t)\, F^*(t)\, \theta(t-4m_\pi^2)$

$\rho(t) = \sqrt{1-4m_\pi^2/t}$ phase space

In the elastic region

$$\frac{1}{2i}\left[F(t+i\varepsilon) - F(t-i\varepsilon)\right] = \frac{1}{2i}\left(\exp(2i\delta_1^1(t)) - 1\right) F^*(t)$$

How so? Unitarity for partial wave amplitudes.

Digression: $f_1^1(t) = \dfrac{1}{2i\rho(t)}\left[\exp(2i\delta_1^1(t)) - 1\right]$

$$= \frac{1}{2i\rho(t)}\left[\cos 2\delta_1^1(t) + i\sin 2\delta_1^1(t) - 1\right]$$

$$= \frac{1}{2i\rho(t)}\left[-2\sin^2\delta_1^1(t) + 2i\sin\delta_1^1(t)\cos\delta_1^1(t)\right]$$

$$\left.\begin{aligned} \mathrm{Re}\, f_1^1(t) &= \frac{1}{\rho(t)}\sin\delta_1(t)\cos\delta_1^1(t) \\ \mathrm{Im}\, f_1^1(t) &= \frac{1}{\rho(t)}\sin^2\delta_1^1(t) \end{aligned}\right\}$$

More common elastic formula

$f_1^1(t) = \dfrac{1}{\rho(t)}\, e^{i\delta_1^1(t)} \sin\delta_1^1(t)$

$$|f_1^1(t)|^2 = \frac{1}{\rho(t)^2}\sin^2\delta_1^1(t)\left[\cos^2\delta_1(t) + \sin^2\delta_1(t)\right]$$

$$= \frac{1}{\rho(t)}\,\mathrm{Im}\, f_1^1(t)$$

q - magnitude of c.m. 3 momentum

If we write η_J as an exponential, and for convenience put

$$\eta_J = e^{-2\rho_J} \tag{4.162}$$

where ρ_J is real and positive, then

$$f_J = \frac{e^{2i(\delta_J + i\rho_J)} - 1}{2iq}. \tag{4.163}$$

The effect of the inelastic channels has been to give the phase-shift a positive imaginary part.

The Argand diagram provides an elegant way of describing the energy dependence of a partial wave amplitude f_J. Eq. (4.161) may be written in the form

$$2qf_J = i(1 - \eta_J e^{2i\delta_J})$$

where δ_J and η_J are functions of the energy or of the momentum q. As the energy varies the locus of $2qf_J$ on the Argand diagram cannot move outside the circle of unit radius with point (0,1) as centre. For $\eta_J = 1$, $2qf_J$ lies on the circle, this corresponds to a fully elastic process; as we pass the threshold for inelastic processes, η_J becomes less than one and the locus moves in from the circle. A typical plot is shown in Fig. 4.7. The locus starts at the point O

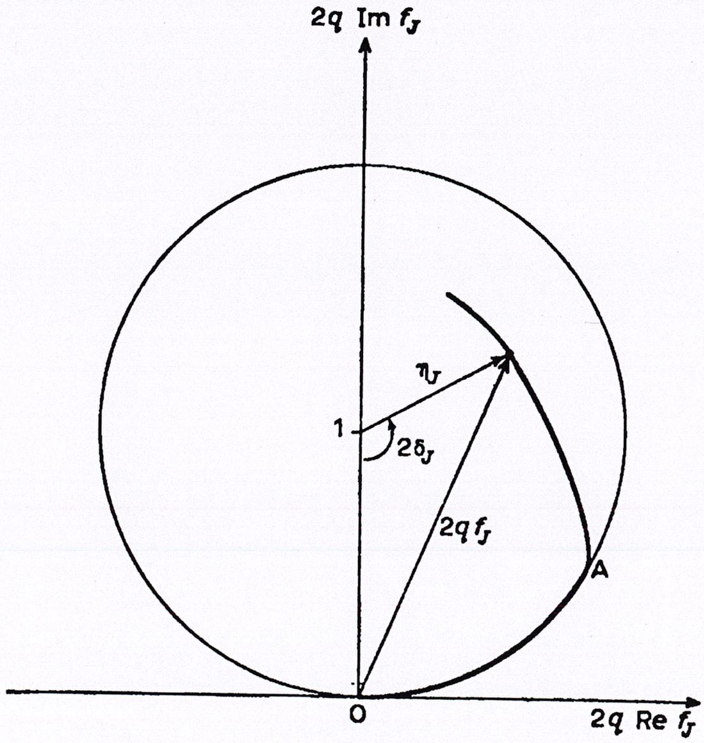

Fig. 4.7. Argand diagram of $2qf_J$.

More generally $f^I_\ell(s) = \dfrac{\eta^I_\ell(s)\, e^{2i\delta^I_\ell(s)} - 1}{2i\rho(s)}$

elasticity parameter $\longrightarrow \eta^I_\ell = e^{-2\beta^I_J}$

Argand plot $\quad \underline{\lfloor 2a_I f^I_\ell}$

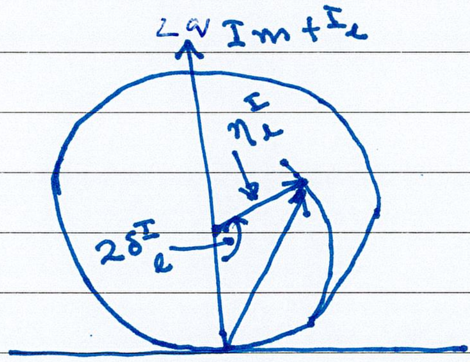

$\mathrm{Im}\, f^I_\ell(s)$

$\geqslant \rho(s)\, |f^I_\ell(s)|^2$

Positivity.

Where does all this stem from?

From unitarity relation, projection on to partial waves and orthogonality properties of Legendre polynomials.

Recall relation before the above

$$\mathrm{Im}\, T(s, \cos\theta) = (\ ) \int d\Omega' \langle 0\, 0 | T | \theta' \varphi' \rangle^* \langle \theta' \varphi' | T | \theta\, \varphi \rangle$$

$4m^2 \leq s \leq 16m^2$

When expressed as an integral over t' and t''

$$1 + \frac{t'}{2q^2} = \cos\theta'$$

$$1 + \frac{t''}{2q^2} = \cos\theta'' = \cos\theta' \cos\theta + \sin\theta' \sin\theta \cos\varphi'$$

$$\mathrm{Im}\, T(s,t) = (\ ) \int dt'\, dt''\, \Theta(J)\, J^{-1/2}\, T^*(s,t')\, T(s,t'')$$

$$J(s,t,t',t'') = \left[\frac{t\, t'\, t''}{q^2} + 2\,(t t' + t t'' + t' t'') - t^2 - t'^2 - t''^2 \right]$$

Kibble

Jacobian of the transformation

2-body unitarity crucial for determining the boundaries of the Mandelstam rep.

End of digression

Rusche & Woolcock general derivation

Returning to the unitarity relation for form factor

$\varepsilon \to 0$ $\quad F(t) - F^*(t) = (e^{2i\delta_1^1(t)} - 1)\, F^*(t)$

$t \in \mathbb{R}$

$$\Rightarrow \quad F(t) = e^{2i\delta_1^1(t)}\, F^*(t)$$

$$\text{But} \quad F(t) = |F(t)|\, e^{i\varphi(t)}$$

Fermi-Watson theorem. $\quad \Rightarrow \quad \varphi(t) = \delta_1^1(t) \bmod k\pi$

$$\ln F(t+i\varepsilon) - \ln F(t-i\varepsilon) = 2i\varphi(t)$$

$$t \geq 4m_\pi^2$$

Logarithm is singular when $F(t)$ has a zero

Find a polynomial $P(t)$ with same set of zeros.

Define $\Omega(t) = F(t) / P(t)$

$$\ln \Omega(t+i\varepsilon) - \ln(t-i\varepsilon) = \ln F(t+i\varepsilon) - \ln(t-i\varepsilon)$$

Now write a dispersion relation with a subtraction at $t=0$

$$\ln \Omega(t) = \ln \Omega(0) + \frac{t}{\pi} \int_{4m^2}^{\infty} \frac{\varphi(t')}{t'(t'-t)} dt'$$

Take $\Omega(t) = \exp\left(\frac{t}{\pi} \int \frac{dt' \, \varphi(t')}{t'(t'-t)} \right)$

Omnès function

$\Omega(t)$ asymptotically $t^{-\varphi(\infty)/\pi}$ [Barton]

Levinson $F(t) \sim t^{\,n - \varphi(\infty)/\pi}$ n – # of zeros

We now need to write down dispersion relations for scattering amplitudes.

When we had only S- and P-wave imaginary parts, each of the w_i (chiral) could be written as a dispersion integral. Simple and also related to subtractions.

In general more complicated: $T_S(s,t,u)$ need to deal with 2 variables. Let us fix one: t (≤ 0). s-channel imaginary part $s \geq 4m^2$ $\pi\pi$, 4π, $K\bar{K}$ ...

Plane has a cut $(4m^2, \infty)$ [right-hand]

What about other cuts? F.F. had none.

We will now have $(-t, \infty)$ due to particle production in the crossed-channel

Crossing symmetry: Amplitude can be analytically continued from physical region $s \geq 4m^2$, $t \leq 0$ to complex values of variables

Same analytical function describes the crossed channels.

General analytic structure at fixed-t

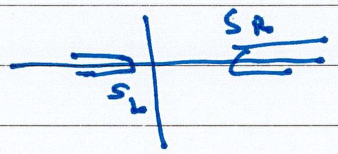

Froissart bound

$$\sigma_{tot}(s) < C \ln(s/s_0)^2$$

$$C = \frac{\pi}{m_\pi^2} \text{ for } \pi-\pi$$

$$|T(s,t)|_{t\le 0} < C' s \, (\ln s/s_0)^2$$

After identifying the cuts we set up d.r.

Subtractions?

Dispersion Relations (book of Irinel Caprini)

Mathematically most straightforward way to exploit analyticity - Cauchy's Theorem

Assume no poles (bound states) on 1^{st} Riemann sheet

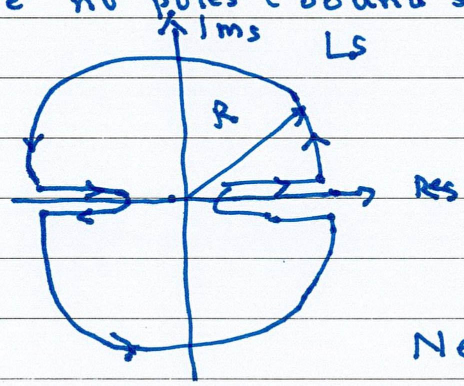

fixed-t

$$T(s,t) = \frac{1}{2\pi i} \oint \frac{T(s',t)}{s'-s} ds'$$

Neglect cont from circle

Schwarz, discontinuity

$$T(s,t) = \frac{1}{\pi} \int_{-\infty}^{s_L} \frac{\mathrm{Im}\, T(s'+i\varepsilon, t)}{s'-s} ds' + \frac{1}{\pi} \int_{s_R}^{\infty} \frac{\mathrm{Im}\, T(s'+i\varepsilon, t)}{s'-s} ds'$$

$$\frac{1}{z \pm i\varepsilon} = P\left(\frac{1}{z}\right) \mp i\pi\delta(z) \qquad \text{Plemelj relation}$$

as s approaches the real axis, write a Hilbert transform

$$\mathrm{Re}\,T(s,t) = \frac{1}{\pi}\int_{-\infty}^{s_L} \frac{\mathrm{Im}\,T(s'+i\varepsilon,t)}{s'-s}\,ds' + \frac{1}{\pi}\underbrace{P\int_{s_R}^{\infty}}_{\text{Cauchy PV}} \frac{\mathrm{Im}\,T(s'+i\varepsilon,t)}{s'-s}\,ds'$$

Dispersion relation (analogous to Kramers-Krönig)

Extend the analogy $\mathrm{Im}\,T(s,t)$ $s > s_R$

absorptive part $A_s(s,t)$ in s-channel

Absorptive parts evaluated at upper-rim of cut.

$\mathrm{Im}\,T(s,t)$ $s < s_L$

absorptive part $A_u(s,t)$ in u-channel

$$T(s,t) = \frac{1}{\pi}\int_{-\infty}^{s_L} \frac{A_u(s'+i\varepsilon,t)\,ds'}{s'-s} + \frac{1}{\pi}\int_{s_R}^{\infty} \frac{A_s(s'+i\varepsilon,t)\,ds'}{s'-s}$$

can be subtracted at some s_1

$$T(s,t) = T(s_1,t) + \frac{1}{\pi}\int_{-\infty}^{\infty} \frac{A_u(\quad)}{(s'-s)(s'-s_1)} + \ldots$$

the symmetry of an amplitude does not require specific assumptions on its asymptotic behaviour in the complex plane.

Suppose that $T(s)$ is symmetric $(T(-s)=T(s))$ and satisfies twice-subtracted dispersion relations. We perform the subtractions at $s=0$:

$$T(s)=T(0)+\frac{s^2}{\pi}\int_{s_0}^{\infty}\mathrm{d}s'\,\frac{A(s')}{s'^2}\left[\frac{1}{s'-s}+\frac{1}{s'+s}\right]. \tag{A.1}$$

Rewriting (A.1) for $s=s_1$, we see after elementary transformations that the difference $T(s)-T(s_1)$ is given by

$$T(s)-T(s_1)=\frac{s-s_1}{\pi}\int_{s_0}^{\infty}\mathrm{d}s'\,A(s')\left[\frac{1}{(s'-s)(s'-s_1)}-\frac{1}{(s'+s)(s'+s_1)}\right]. \tag{A.2}$$

This is a once-subtracted dispersion relation with arbitrary subtraction point s_1.

Similarly, suppose that $T(s)$ is antisymmetric $(T(-s)=-T(s))$ and satisfies once-subtracted dispersion relations. Subtracting at $s=0$, we have

$$T(s)=\frac{s}{\pi}\int_{s_0}^{\infty}\mathrm{d}s'\,\frac{A(s')}{s'}\left[\frac{1}{s'-s}+\frac{1}{s'+s}\right]. \tag{A.3}$$

It is immediately seen that this relation may be transformed into the unsubtracted dispersion relation

$$T(s)=\int_{s_0}^{\infty}\mathrm{d}s'\,A(s')\left[\frac{1}{s'-s}-\frac{1}{s'+s}\right]. \tag{A.4}$$

Appendix B

Interchange of differentiation with respect to t and integration over s.

For definiteness we consider the integral

$$J(t)=\int_{4}^{\infty}\mathrm{d}s\,\frac{1}{s^2}\,A^{(1)}(s,t) \tag{B.1}$$

Mandelstam Representation and reduction to single variable.

Mandelstam analyticity expressed by the equation

$$T^{I}(s,t,u) = \frac{1}{\pi^2}\int_4^\infty ds' \int_4^\infty dt' \frac{\rho^{I}_{st}(s',t')}{(s'-s)(t'-t)} + s \to u + t \to u$$

Boundaries of the support of ρ_{st} given by the Kibble function

$$(s-4)(t-16) - 64 = 0$$
$$(t-4)(s-16) - 64 = 0$$

Analogously for ρ_{tu} and ρ_{su}

We obtain familiar results on analytic properties of $T^{I}(s,t,u)$ with one-variable (t) fixed

Will converge for $-32 < t < 4$

Bring to 'canonical' form

$$T^{I}(s,t,u) = \frac{1}{\pi}\sum_{I'}\int_4^\infty ds' \, \mathrm{Im}\, T^{I'}(s,t) \times \left[\frac{\delta_{II'}}{s'-s} + \frac{C^{su}_{II'}}{s'-u} \right]$$

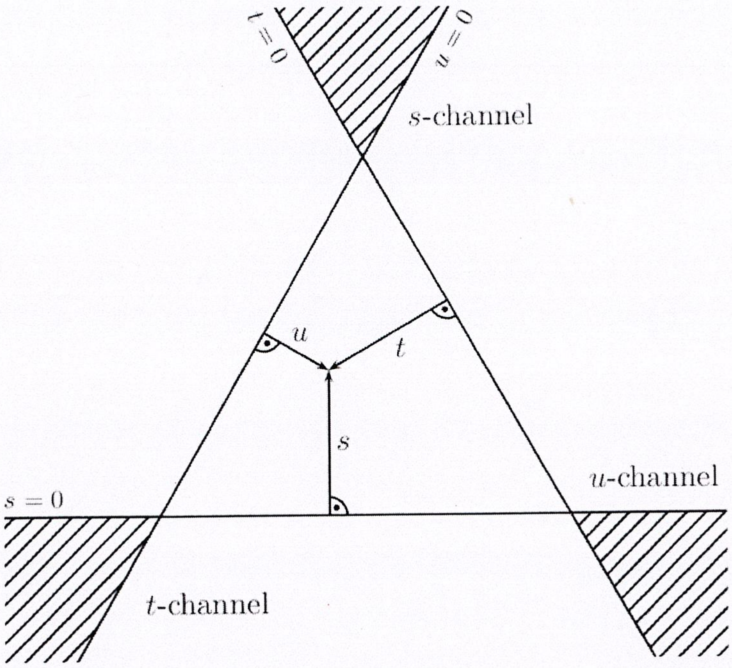
t = 0
u = 0
s-channel
u
t
s
s = 0
u-channel
t-channel

and that t_L increases as either t_1 or t_2 increases. Therefore the minimum value of t_L, say $t_L = b(s)$, is obtained by taking the lowest values of t_1 and t_2 occurring in the integration of eq. (6.81), that is $t_1 = t_2 = 4m^2$. Now

$$K(s, t; 4m^2, 4m^2) = t\left(t - 16m^2 - \frac{16m^4}{q^2}\right)$$

and so, taking the larger root, we have

$$(t_L)_{\min} \equiv b(s) = 16m^2 + \frac{16m^4}{q^2}. \tag{6.86}$$

The boundary curve of the double spectral function $\rho_{st}(s, t)$ is therefore given by $t = b(s)$. Note that this curve, which is shown in Fig. 6.5, is asymptotic to the lines $s = 4m^2$ and $t = 16m^2$. From eqs. (6.81), (6.82) and (6.84) we find for $t > b(s)$ that

$$\rho_{st}(s, t) = \frac{1}{4Wq} \int_{4m^2} \mathrm{d}t_1 \int_{4m^2}^{K(s,t;t_1,t_2)=0} \mathrm{d}t_2 \frac{D_t(s, t_1)\, D_t^*(s, t_2)}{[K(s, t; t_1, t_2)]^{\frac{1}{2}}} \tag{6.87}$$

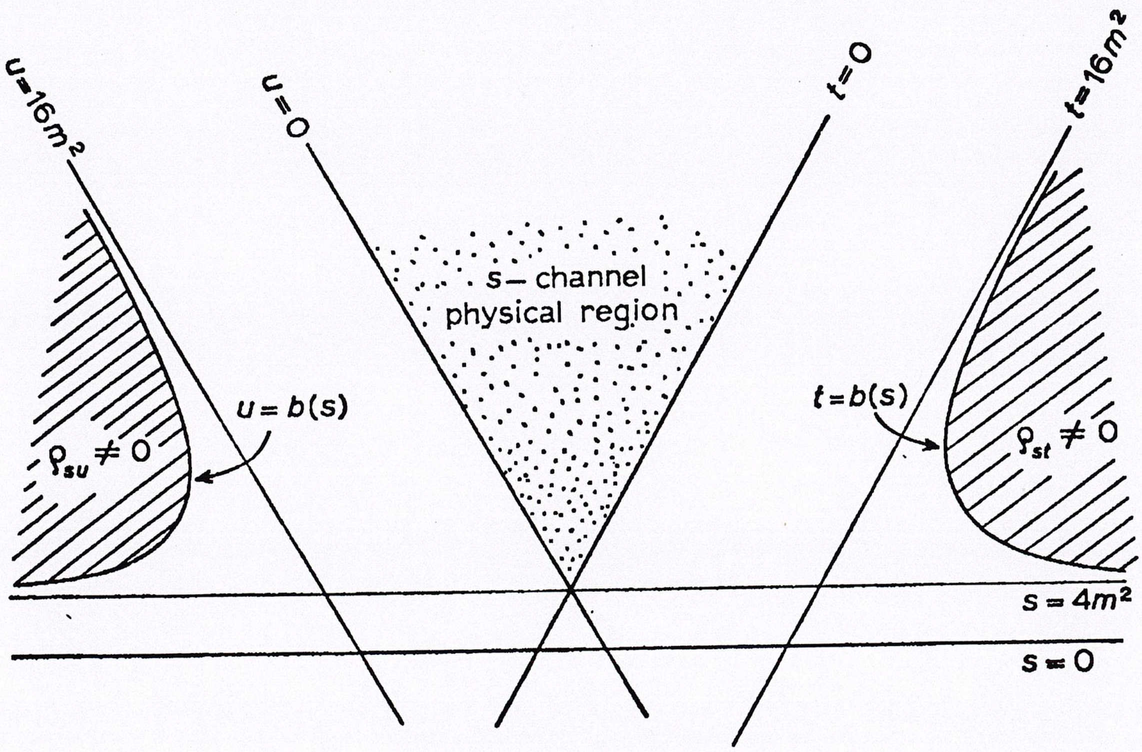

Fig. 6.5. The Mandelstam diagram for $\pi\pi$ scattering, showing the elastic s-channel double spectral functions.

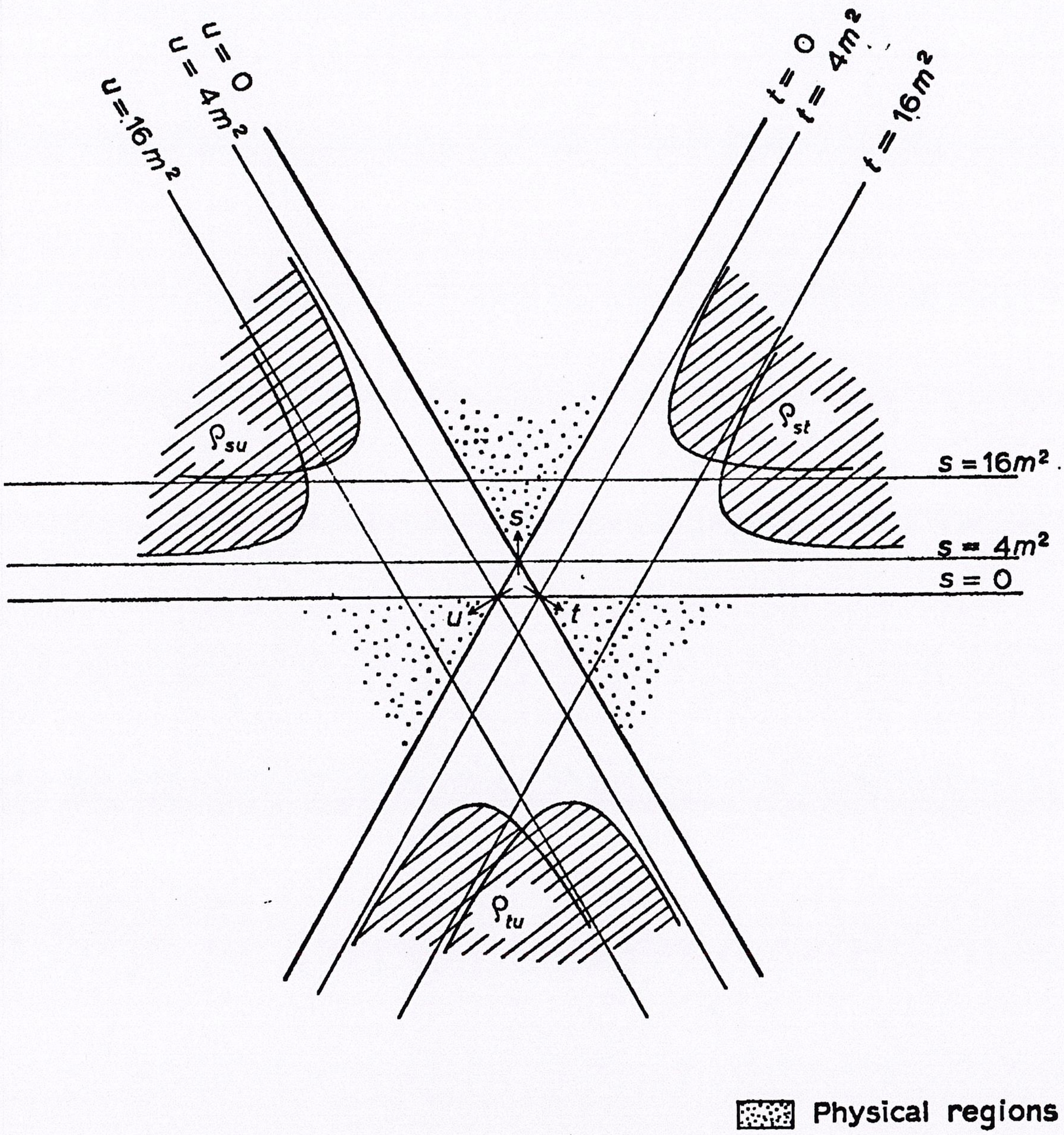

Fig. 6.6. The double spectral functions (shaded) for $\pi\pi$ scattering.

unitarity in each of the three channels, and consequently we speak of maximum analyticity of the amplitude. This double spectral representation was originally postulated by MANDELSTAM [1958] and is known as the Mandelstam representation.

No general 'proof' of the Mandelstam representation is known. An approach, which has been partially successful, is to study the singularity structure of Feynman diagrams. LANDAU [1959] has shown that for an arbitrary diagram these singularities occur for values of the external variables (such as s, t) that allow the internal particle momenta to be on their mass shells. Many low order diagrams have been studied in this way and are found to satisfy the Mandelstam representation. However the general